Index Modulated OFDM with ICI Self-Cancellation for V2X Communications

Yuke Li[1,2], Miaowen Wen[3], Xiang Cheng[2,4], and Liu-Qing Yang[1,2,5]

[1]State Key Laboratory of Management and Control for Complex Systems,
Institute of Automation, Chinese Academy of Sciences, Beijing 100190, China

[2]Qingdao Academy of Intelligent Industries, Qingdao, 266109, China.

[3]School of Electronic and Information Engineering,
South China University of Technology, Guangzhou 510640, China

[4]School of Electronics Engineering and Computer Science, Peking University, Beijing, 100871, China

[5]Department of Electrical and Computer Engineering, Colorado State University, Fort Collins, CO 80523, USA

Email: liyuke14@mails.ucas.ac.cn, eemwwen@scut.edu.cn, xiangcheng@pku.edu.cn, liuqing.yang@ieee.org.

Abstract— **Recent years have witnessed the rapid development of intelligent transportation systems (ITS), which urgently call for highly reliable and effective communication technologies for vehicle-to-vehicle and vehicle-to-infrastructure (V2X) applications. Orthogonal frequency division multiplexing (OFDM) is widely believed to be the most promising candidate among these applications. However, the orthogonality of subcarriers in OFDM can be easily destroyed by the Doppler-induced inter-carrier interference (ICI), which is very common in V2X channels. In this paper, we propose a novel scheme which integrates the ICI self-cancellation technique into the index modulated (IM-) OFDM framework. Via careful designs, the proposed scheme can not only inherit the advantages of IM-OFDM but also suppress the ICI from active subcarriers. Simulations validate that in V2X channels, the proposed scheme significantly outperforms existing IM-OFDM and more importantly shows better performance than the conventional OFDM with ICI self-cancellation without sacrificing the spectral efficiency.**

I. INTRODUCTION

V2X communications plays an important role in intelligent transportation systems (ITS) by helping "extend a vehicle field of vision", and it is also an indispensable component in vehicular networking [1]. In smart cities, it is expected that vehicles can communicate not only with neighboring vehicles, but also with roadside infrastructures, traffic management centers, and gas/charging stations, etc. Such rapidly growing needs urgently call for communication technologies with high reliability, information availability, fidelity and spectral efficiency [2]. These requirements, together with the high mobility of vehicles, make the V2X communications very challenging.

OFDM is widely believed to be the most promising communication technology for vehicle communications [3], [4], which is evidenced by the worldwide adoption of the IEEE802.11p [5]. However, the orthogonality between subcarriers can be damaged by the Doppler shift, which is very common in V2X communications. The damage of subcarrier orthogonality leads to ICI, which will seriously deteriorate the system performance. Therefore, to ensure the reliability and effectiveness of V2X communication, it is very necessary to suppress ICI to an acceptable level. Several ICI countermea-sures have been proposed in the literature, including frequency offset correction [6]–[8], time-domain windowing [9], and ICI self-cancellation [10], [11]. Among them, ICI self-cancellation has attracted much more attention due to its simplicity and effectiveness in ICI reduction [12], [13]. The main idea of ICI self-cancellation is that a pair of data symbols with opposite polarity are modulated onto two adjacent subcarriers, thus the ICI signals generated within adjacent subcarriers can be self-canceled each other.

The power of ICI is largely scaled with the number of active subcarriers. It is natural to expect that the ICI level could be reduced by inactivating some subcarriers. However, this mea-sure comes at the cost of spectral efficiency because nothing is transmitted by the idle subcarriers. A recently emerging technique, called IM-OFDM in this paper, is a candidate to solve the aforementioned problem due to its potential of striking an attractive trade off between the number of active subcarriers and spatial spectral efficiency. It is inspired by the idea of spatial modulation, which belongs to the multi-input-multi-output (MIMO) family and is widely accepted as a candidate for 5G transmission techniques [14]–[16]. Different from conventional OFDM, IM-OFDM renders partial subcarriers to be idle and selects them randomly according to spatial modulation. Therefore, in IM-OFDM, the information is conveyed not only by the M-ary signal constellation as in conventional OFDM but also by the indices of the inactive subcarriers. It has been verified that IM-OFDM can achieve significantly better bit error performance than conventional OFDM under different channel conditions in the absence of the frequency offset [17]. The advantages of IM-OFDM have spawned a great number of further researches. Being aware that the method proposed in [17] for subcarrier grouping is suboptimal in the sense of BER performance, we suggested grouping subcarriers in an interleaved manner instead and got significant performance improvement [18]. On the other hand, our analysis from an information-theoretic perspective verified that the interleaved grouping is optimal for IM-OFDM in the sense of achievable rate [19]. For above reasons, we will

refer to IM-OFDM as the IM-OFDM system with interleaved grouping in this paper.

Owing to the fact that partial subcarriers are inactive and active subcarriers are separated in frequency to some extent, IM-OFDM is expected to have the potential of ICI suppression. However, in the presence of Doppler shift, the ICI largely contributes to the power of the received signals at inactive subcarriers and in turn misleads the detection of subcarrier states. The incorrect detection of subcarriers states results in not only the incorrect estimation of the information bits conveyed by the indices of active subcarriers but also the incorrect demodulation of the M-ary PSK/QAM symbols, making the ICI suppression potential submerged in the deteriorated system performance. This may result in IM-OFDM expressing significantly decreased performance and loses its competitiveness compared to conventional OFDM with ICI self-cancellation when applied to V2X communications. Therefore, how to properly deal with ICI is also a very important issue for IM-OFDM and still an open research problem.

To fill the aforementioned gap, in this paper, inspired by the properties of IM-OFDM, we for the first time redesign ICI self-cancellation and propose a scheme which seizes both merits of IM-OFDM and ICI self-cancellation [20]. The developed IM-OFDM with ICI self-cancellation scheme is simple yet effective and performs a better system performance than IM-OFDM as well as ICI self-cancellation. To better demonstrate the idea, we perform the simulations over V2X channels for 6 different scenarios. It is shown through analysis that in the proposed scheme, the ICI caused by Doppler shift can be suppressed to a very low level with the help of ICI self-cancellation and spatial modulation. Simulations over different scenarios reveal that the proposed scheme significantly outperforms existing IM-OFDM in the entire SNR region and OFDM with ICI self-cancellation when BER falls below 10^{-2}. More importantly, the SNR gain over OFDM with ICI self-cancellation is up to 5 dB.

II. PROPOSED SCHEME

Suppose that there are in total N OFDM subcarriers. In the proposed scheme, they are divided into G groups, of which each contains $2L$ subcarriers. Therefore, $N = 2GL$. Note that in the proposed scheme, two adjacent subcarriers are considered as one subcarrier pair. Thus, each group contains L subcarrier pairs. Denote the index of the l-th subcarrier pair within g-th group as $\beta_{g,l}$, where $g = 1, 2, \cdots, G$ and $l = 1, 2, \cdots, L$. In each pair of subcarriers, the index of one subcarrier is denoted by $\beta_{g,l}^1$, and the other $\beta_{g,l}^2$, such that $\beta_{g,l} = \{\beta_{g,l}^1, \beta_{g,l}^2\}$.

A. Transmitter structure

Fig. 1 shows the transmitter structure of the proposed scheme. For each group, only m out of L subcarrier pairs are set to be active to transmit modulated symbols and the remaining $L - m$ subcarrier pairs are set to be idle. It is worth noting that the subcarrier state is determined pair-wise in the proposed scheme, which means, the two neighboring subcarriers within one subcarrier pair share the same state.

Therefore, for each group, there will be $C(L, m)$ kinds of combinations which consist of the indices of active subcarrier pairs. Thus, $p_1 = \lfloor \log_2 C(L, m) \rfloor$ bits can be conveyed by subcarrier activation, where $C(\cdot, \cdot)$ denotes the binomial coefficient and $\lfloor \cdot \rfloor$ returns the maximal integer less than the argument. In each group, the first coming p_1 bits determine the index combination of active/inactive subcarrier pairs. The determination can be implemented via either the look-up table method or the combinatorial method. Details about how both methods work can be found in [17]. Denote the determined index combination for subcarrier group g as I_g, which is comprised of the indices of active subcarrier pairs.

Next, the modulated symbols are drawn from the M-ary PSK/QAM constellation and then assigned to the active subcarrier pairs, where M is the cardinality of the constellation. Due to the fact that the difference between ICI coefficients of adjacent subcarriers is very small, the ICI signal is expected to be self-canceled within adjacent subcarriers. Therefore, a data pair with opposite polarity, such as $(a, -a)$, is modulated onto two adjacent subcarrier $\{\beta_{g,l}^1, \beta_{g,l}^2\}$, where $\beta_{g,l} \in I_g$. By this design following the ICI self-cancellation technique [10], the ICI generated by $\beta_{g,l}^2$-th subcarrier is expected to be cancelled out by that generated by $\beta_{g,l}^1$-th subcarrier. Since $m \log_2 M$ bits can be conveyed by symbol modulation, by taking subcarrier activation and M-ary modulation into account, each subcarrier group conveys $\lfloor \log_2 C(L, m) \rfloor + m \log_2 M$ bits. Thus, the spectral efficiency achieve by the proposed system is (bps/Hz):

$$f_{Proposed} = \frac{\lfloor \log_2 C(L, m) \rfloor}{2L} + \frac{m \log_2 M}{2L}. \quad (1)$$

We consider interleaved grouping for its optimality among all possible subcarrier grouping methods. Different from the manner adopted in conventional IM-OFDM, in the proposed scheme the subcarriers are grouped in pairs. Equal-spaced subcarrier pairs in frequency are collected to form a group:
$$\{\beta_{1,1}, \beta_{2,1}, \cdots, \beta_{G,1}, \beta_{1,2}, \beta_{2,2}, \cdots, \beta_{G,2}, \cdots, \beta_{1,L}, \beta_{2,L},$$
$$\cdots, \beta_{G,L}\} = \left\{ \bigcup_{g=1}^{G} \beta_{g,1}, \bigcup_{g=1}^{G} \beta_{g,2} \cdots, \bigcup_{g=1}^{G} \beta_{g,L} \right\}.$$

Denote the transmitted signals in the frequency domain as $x(k)$, where $k = 1, 2, \ldots, N$. The transmitted signals at all subcarriers of the proposed system are given by
$$\mathbf{X} = [x(1), \ldots, x(N)]^T = \left[\bigcup_{g=1}^{G} s_{\beta_g,1}, \cdots, \bigcup_{g=1}^{G} s_{\beta_g,L} \right]^T, \quad (2)$$

where $s_{\beta_g,l}$ denotes the $\beta_{g,l}$-th pair of transmitted signals, $s_{\beta_g,l} = \{s_{\beta_{g,l}^1}, s_{\beta_{g,l}^2}\}$, and $(\cdot)^T$ stands for the transpose operation. Before transmission, the inverse fast Fourier transform (IFFT) is applied to (2). Then, a cyclic prefix (CP) is added to the beginning of the time-domain OFDM symbol.

B. Receiver structure

Fig. 2 shows the receiver structure of the proposed scheme. At the receiver, the CP of the received signal is first removed and the application of the FFT is followed. The received signal at the k-th subcarrier can be expressed as:
$$y(k) = h(k)x(k)C(0) + \sum_{i=1, i \neq k}^{N} h(i)x(i)C(i - k) + w(k), \quad (3)$$
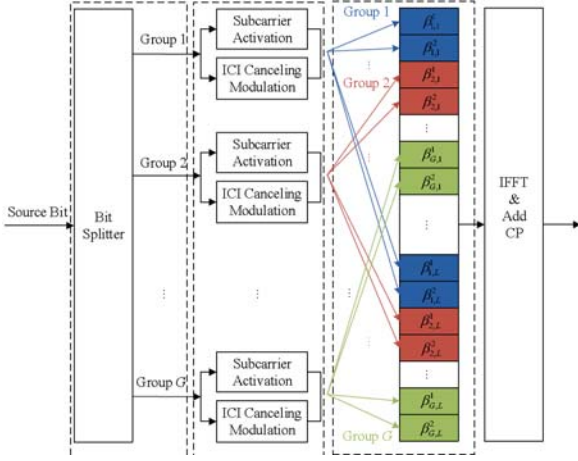
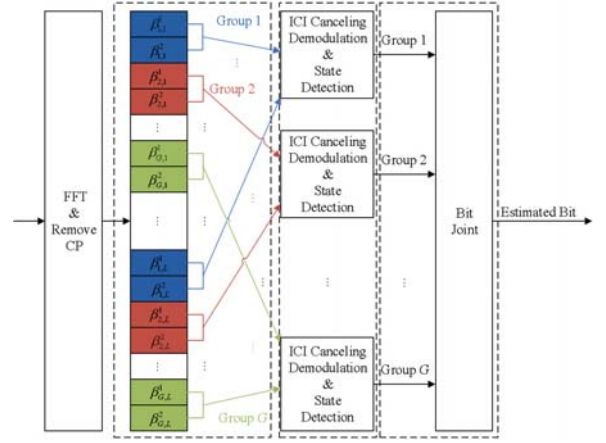Fig. 1.   Transmitter structure of the proposed scheme.

Fig. 2.   Receiver structure of the proposed scheme.

where $h(k)$ and $w(k)$ represent the channel frequency response and the noise at the k-th subcarrier respectively, where $k = 1, 2, \cdots, N$. The second term at the right-hand side of (3) represents the ICI, where $C(i-k)$ is the ICI coefficient, given by

$$C(i-k) = \frac{\sin(\pi(i+\varepsilon-k))}{N\sin(\frac{\pi}{N}(i+\varepsilon-k))} \cdot \exp\left(\frac{j\pi(N-1)(i+\varepsilon-k)}{N}\right), \quad (4)$$

with ε denoting the normalized CFO to the subcarrier spacing.

Denote the $\beta_{g,l}$-th received signal pair as $r_{\beta_{g,l}} = \left\{r_{\beta_{g,l}^1}, r_{\beta_{g,l}^2}\right\}$. The received signals at all subcarriers of the proposed system are given by

$$\mathbf{Y} = [y(1), \ldots, y(N)]^T = \left[\bigcup_{g=1}^{G} r_{\beta_{g,1}}, \cdots, \bigcup_{g=1}^{G} r_{\beta_{g,L}}\right]^T. \quad (5)$$

Next, all received signals are grouped in an interleaved manner similar to the operations performed at the transmitter. That is, all received signals are extracted as: $\left\{r_{\beta_{1,1}}, r_{\beta_{1,2}}, \cdots, r_{\beta_{1,L}}, \cdots\cdots, r_{\beta_{G,1}}, r_{\beta_{G,2}}, \cdots, r_{\beta_{G,L}}\right\} = \left\{\bigcup_{l=1}^{L} r_{\beta_{1,l}}, \cdots, \bigcup_{l=1}^{L} r_{\beta_{G,l}}\right\}$. Then, the ICI canceling demodulation is executed within each pair of subcarriers, yielding

$$r'_{\beta_{g,l}} = \frac{1}{2}(r_{\beta_{g,l}^1} - r_{\beta_{g,l}^2}). \quad (6)$$

In this manner, the residual ICI in the received signals can be reduced further.

The joint detection of the subcarriers states and the modulated symbols is carried out based on the maximum-likelihood (ML) criterion. The ML detector considers all possible realizations by searching for all possible subcarrier index combinations and signal constellation points to make a joint decision on the combination of active indices and the constellation symbols, denoted as $\hat{I}_g$ and $\hat{S}_g$ respectively. For group g, there are $\mathrm{C}(L,m)$ kinds of index combinations of active subcarriers, denoted by Φ_b^g, where $b = 1, 2, \cdots, \mathrm{C}(L,m)$. Let $\bar{\Phi}_b^g$ denote the complement of Φ_g^b. The ML detector can be derived as:

Scenario	Velocity (km/h)	Doppler Shift (Hz)
Scenario 1	104	1000-1200
Scenario 2	32-48	300
Scenario 3	104	900-1150
Scenario 4	104	600-700
Scenario 5	32-48	400-500
Scenario 6	32-48	300-500

$$\left\langle\hat{I}_g, \hat{S}_g\right\rangle = \arg\min_{b\in\Theta} \sum_{\beta_{g,l}\in\Phi_b^g}\left|r'_{\beta_{g,l}} - h'_{\beta_{g,l}}\hat{s}_{\beta_{g,l}}\right|^2 + \sum_{\beta_{g,l}\in\bar{\Phi}_b^g}\left|r'_{\beta_{g,l}}\right|^2, \quad (7)$$

where $\Theta = \{1, 2, \cdots, \mathrm{C}(L,m)\}$ and $\hat{s}_{\beta_{g,l}}$ is the estimated transmitted signal carried on the $\beta_{g,l}$-th subcarrier pair, which can be gotten by searching for the closest constellation point to $r'_{\beta_{g,l}}$, and $h'_{\beta_{g,l}}$ is the channel frequency response at the $\beta_{g,l}$-th subcarrier pair, defined as $h'_{\beta_{g,l}} = \frac{1}{2}\left(\hat{h}_{\beta_{g,l}^1} + \hat{h}_{\beta_{g,l}^2}\right)$, where $\hat{h}_{\beta_{g,l}^1}$ and $\hat{h}_{\beta_{g,l}^2}$ represent the channel estimates on the corresponding subcarriers. Details about the implementation of the detector are presented in [20].

Remark 1: It is clear that the computation of the proposed detector lies in (6) and (7). Since only $N/2$ data are to be demodulated, the contributed computational complexity by (6) is on the order of $\mathcal{O}(N)$. Since (7) has to search through all possible combinations of active subcarrier indices, the contributed computational complexity is on the order of $\mathcal{O}(\mathrm{C}(L,m))$ per group. Taking all groups into account, the total computational complexity of the proposed detector amounts to $\mathcal{O}(N + G\mathrm{C}(L,m))$. Recall that the computational complexity of the exiting IM-OFDM scheme applying log-likelihood ratio (LLR) detector is about $\mathcal{O}(N + G\mathrm{C}(L,m))$ [17]. It can be concluded that the proposed scheme achieves nearly the same computational complexity as the existing IM-OFDM scheme.

III. CHANNEL MODEL AND ESTIMATION

So far, V2X channels have been extensively investigated. In the simulations, we adopt the channel model proposed in [22] and [23], which typically regarded as a standard V2X

TABLE II

SYSTEM PARAMETERS

Parameter	Value
Signal Bandwidth	10 MHz
Carrier Frequency	5.9 GHz
Number of Total Subcarriers	64
Number of Cyclic Prefix	16
Subcarrier Spacing	156.3 kHz
OFDM Symbol Duration	8 μs

channel model dedicated for IEEE 802.11p. The measurement campaign was carried out in the metropolitan Atlanta, Georgia area including six scenarios, which are

- Scenario 1: V2V Expressway Oncoming;
- Scenario 2: V2V Expressway Same Direction with Wall;
- Scenario 3: V2V Urban Canyon Oncoming;
- Scenario 4: Roadside-to-vehicle (R2V) Expressway;
- Scenario 5: R2V Urban Canyon Oncoming; and
- Scenario 6: R2V Suburban Street.

The channel parameters for these six scenarios are listed in Table I. For brevity, we only present the results under Scenario 1, Scenario 3, and Scenario 5, which cover both V2V and R2V channels and a wide range of Doppler shifts.

In the simulations, the channel estimation is performed by the preamble, which is located prior to each OFDM data symbol and comprises an entire OFDM symbol known by both the transmitter and the receiver. Then, the channel estimates are used for the equalization and demodulation of the OFDM data symbol. We measure the BER achieved by the system adopting the ML detector versus the SNR, which is defined as $P/(mN_0)$.

IV. SIMULATION RESULTS AND ANALYSIS

In this section, we carry out Monte Carlo simulation to validate the benefits of the proposed scheme in typical V2X environment. The system parameters are listed in Table II, which are configured according to IEEE 802.11p [5]. The channel parameters are introduced in section III. For the proposed scheme, the system parameters are chosen as: 1) $G = 8$, $L = 4$, $m = 3$, and QPSK modulation; 2) $G = 4$, $L = 8$, $m = 6$ and QPSK modulation. For comparison, we choose

- Scheme 1: OFDM with BPSK modulation;
- Scheme 2: OFDM with ICI self-cancellation and QPSK modulation;
- Scheme 3: IM-OFDM with four subcarriers as a group, two subcarriers activated, and BPSK modulation.

For a fair comparison, we set parameters such that all schemes achieve the same spectral efficiency, i.e., 1 bits/Hz.

Fig. 3 shows the performance differences among Schemes 1-3 and the proposed scheme ($G = 8$, $L = 4$, $m = 3$, and QPSK modulation) under different scenarios. As can be seen, when SNR is low, Scheme 1 and Scheme 2 perform better than the IM-OFDM and the proposed scheme. The reason is that when the SNR is low, the noise largely contributes to the power of received signals. Consequently, the power of the received
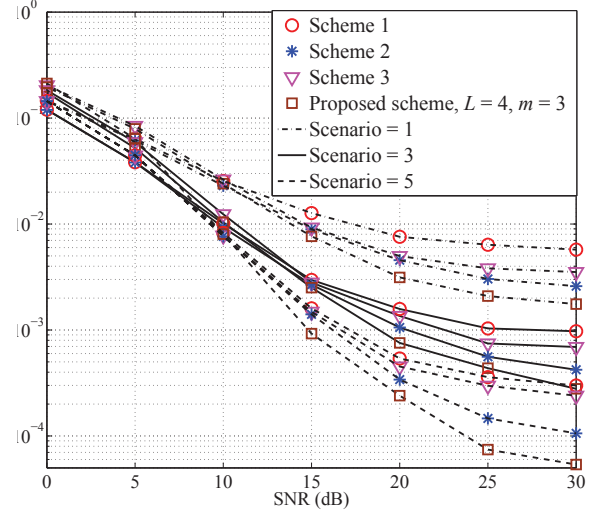

Fig. 3. BER performance comparison for Scenario 1, Scenario 3, and Scenario 5 among Schemes 1-3 and the proposed scheme ($L = 4$, $m = 3$, and QPSK modulation).
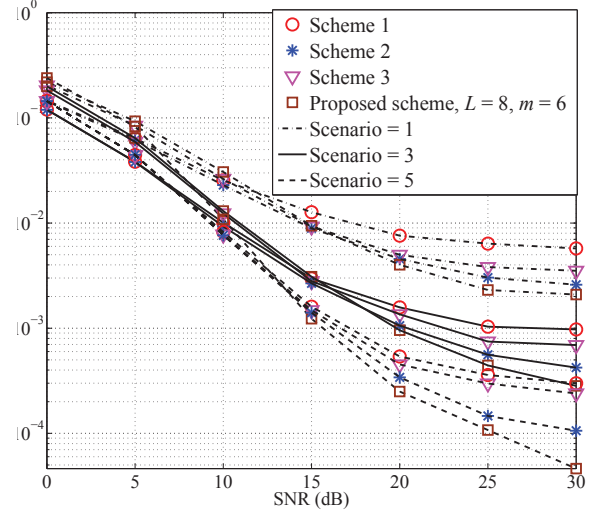

Fig. 4. BER performance comparison for Scenario 1, Scenario 3, and Scenario 5 among Schemes 1-3 and the proposed scheme ($L = 8$, $m = 6$ and QPSK modulation).

signal at each inactive subcarrier becomes comparable to that at each active subcarrier, which also misleads the detection of subcarrier states. To make the proposed scheme more practical, when SNR< 10 dB, all pairs of subcarriers in the proposed scheme can be set as active. In this way, there is no need to do subcarrier states detection at receiver and the proposed scheme is equivalent to the OFDM with ICI self-cancellation scheme, which achieves a better BER performance when SNR is low.

As the SNR increases, it can be seen that IM-OFDM and proposed scheme outperform conventional OFDM. This happens because subcarriers in IM-OFDM and the proposed scheme are grouped in an interleaved manner, as a result, the effect of correlated frequency-selective fading in V2X channels is reduced significantly. However, IM-OFDM performs worse than Scheme 2 and exhibits error floor at 25

dB. It can be understood since that the ICI signals caused by Doppler shift largely deteriorate the system performance of IM-OFDM, while the ICI signals can be suppressed due to the ICI self-cancellation method in Scheme 2. As can be seen in Fig. 3, when BER falls below 10^{-2}, the proposed scheme performs better than conventional OFDM and IM-OFDM under different scenarios, and more importantly, even better than OFDM with ICI self-cancellation. This is as expected because in the proposed scheme, with the ICI self-cancellation technique being integrated into the IM-OFDM frame work, almost $N(L-m)/L$ subcarriers transmit zero energy and the number of active subcarriers which actually incur ICI is reduced to $(m/L)N$. Note that the above-mentioned SNR threshold, i.e., 10 dB, is meaningful since at it the BER value is around 10^{-2}, which is required by most practical systems.

As detailed in Table II, Scenario 1 has the highest Doppler shift. Correspondingly, the BER error floors are the highest for all three schemes. However, it is worth mentioning that, our proposed IM-OFDM with ICI self-cancellation results in the most significant performance boost when the Doppler is relatively high. This is because the as the Doppler-induced ICI becomes dominant, the effect of ICI suppression in the proposed scheme becomes more obvious with the adoption of the ICI self-cancellation technique.

In proposed scheme, the change of symbol modulation size can be offset by the subcarrier activation parameters to maintain the same transmitted information rate. Hence, alternative to the parameter set used to generate Fig. 3, one could use $L = 8$, $m = 6$, and QPSK modulation without affecting the transmitted information rate. The corresponding results are shown in Fig. 4. From Fig. 4, we observe similar phenomenon to Fig. 3.

V. Conclusions

In this paper, we have proposed a novel scheme which merges the both merits of the ICI self-cancellation technique and the IM-OFDM technique in ICI reduction for V2X communications. The transceiver structure of the proposed scheme has been detailed. Through BER simulations, it has been shown that under the same spectral efficiency the proposed scheme performs better than IM-OFDM in the entire SNR region and conventional OFDM with ICI self-cancellation when BER falls below 10^{-2}.

VI. Acknowledgement

References

[1] F. Wang, D. Zeng, and L. Yang, "Smart cars on smart roads: An IEEE intelligent transportation systems society update," *IEEE Pervasive Computing*, vol. 5, no. 4, pp. 68–69, Oct.-Dec. 2006.

[2] F. Qu, F. Wang, and L. Yang, "Intelligent transportation spaces: vehicles, traffic, communications, and beyond," *IEEE Commun. Mag.*, vol. 48, no. 11, pp. 136–142, Nov. 2010.

[3] M. Wen, X. Cheng, J. Wu, L. Yang, and B. Jiao, "Optimal correlative coding for discrete-time OFDM systems," *IEEE Trans. on Veh. Tech.*, vol. 63, no. 2, pp. 987-993, Feb. 2014 .

[4] X. Cheng, L. Yang, and X. Shen, "D2D for Intelligent Transportation Systems: A Feasibility Study," *IEEE Transactions on Intelligent Transportation Systems*, vol. 16, no. 4, pp. 1784-1793, Aug. 2015.

[5] *802.11p-2010 IEEE Standard for Information Technology‡Telecommunications and Information Exchange Between Systems‡Local and Metropolitan Area Networks‡Specific Requirements Part 11*, Wireless LAN Medium Access Control (MAC) and Physical Layer (PHY) Spec, 2010.

[6] J. J. van de Beek, M. Sandell, and P. O. Borjesson, "ML estimation of time and frequency offset in OFDM systems," *IEEE Trans. Signal Process.*, vol. 45, no. 7, pp. 1800–1805, Jul. 1997.

[7] U. Tureli, D. Kivanc, and H. Liu, "Experimental and analytical studies on a high-resolution OFDM carrier frequency offset estimator,"*IEEE Trans. on Veh. Tech.*, vol. 50, no. 2, pp. 629–643, Mar. 2001.

[8] M. Luise, M. Marselli, and R. Reggiannini, "Low-complexity blind carrier frequency recovery for OFDM signals over frequency-selective radio channels," *IEEE Trans. Commun.*, vol. 50, no. 7, pp. 1182–1188, Jul. 2002.

[9] R. Li and G. Stette, "Time-limited orthogonal multicarrier modulation schemes," *IEEE Trans. Commun.*, vol. 43, no. 234, pp. 1269–1272, Jul. 1995.

[10] Y. Zhao, S-G. Haggman, "Intercarrier interference self-cancellation scheme for OFDM mobile communication systems," *IEEE Trans. Commun.*, vol. 49, no. 7, pp. 1185–1191, Jul. 2001.

[11] M. Wen, X. Cheng, X. Wei, B. Ai, and B. Jiao, "A novel effective ICI self-cancellation method," in *Proc. IEEE Globecom'11*, Houston, USA, Dec. 2011.

[12] X. Cheng, Q. Yao, M. Wen, C. X. Wang, L. Song, and B. Jiao, "Wideband channel modeling and ICI cancellation for vehicle-to-vehicle communication systems," *IEEE J. Sel. Areas in Commun.*, vol. 31, no. 9, pp. 434-448, Sept. 2013.

[13] X. Cheng, M. Wen, X. Cheng, D. Duan, and L. Yang, "Effective mirror-mapping-based intercarrier interference cancellation for OFDM underwater acoustic communications," *Ad Hoc Networks (Elsevier)*, to appear.

[14] R. Mesleh, H. Haas, S. Sinanović, C. W. Ahn, and S. Yun, "Spatial modulation," *IEEE Trans. Veh. Tech.*, vol. 57, no. 4, pp. 2228–2241, Jul. 2008.

[15] M. Di Renzo, H. Haas, A. Ghrayeb, S. Sugiura, and L. Hanzo, "Spatial modulation for generalized MIMO: Challenges, opportunities and implementation," *Proc. of the IEEE*, vol. 102, no. 1, pp. 56-103, Jan. 2014.

[16] X. Cheng, X. Hu, L. Yang, I. Husain, K. Inoue, P. Krein, R. Lefevre, Y. Li, H. Nishi, J. Taiber, F. Wang, Y. Cha, W. Gao, Z. Li, "Electrified Vehicles and the Smart Grid: the ITS Perspective," *IEEE Transactions on Intelligent Transportation Systems*, vol. 15, no. 4, pp. 1388-1404, Aug. 2014.

[17] E. Basar, U. Aygolu, E. Panayirci, and H. V. Poor, "Orthogonal frequency division multiplexing with index modulation," *IEEE Trans. Signal Process.*, vol. 61, no. 22, pp. 5536-5549, Nov. 2013.

[18] X. Cheng, M. Wen, L. Yang, and Y. Li, "Index Modulated OFDM with Interleaved Grouping for V2X Communications," in *Proc. IEEE ITSC 2014*, Qingdao, China, Oct. 2014, pp. 1097-1104.

[19] M. Wen, X. Cheng, and L. Yang, "Optimizing the Energy Efficiency of OFDM with Index Modulation," in *Proc. IEEE ICCS 2014*, Macau, China, Nov. 2014, pp. 31-35.

[20] Y. Li, M. Wen, X. Cheng, and L. Yang, "Index modulated OFDM with ICI self-cancellation," submitted to *Proc. IEEE VTC 2016*, Nanjing, China, May 2016.

[21] M. Wen, X. Cheng, M. Wang, B. Ai, and B. Jiao, "Error probability analysis of interleaved SC-FDMA systems over Nakagami-m frequency selective fading channels," *IEEE Trans. Veh. Technol.*, vol. 62, no. 2, pp. 748–761, Feb. 2013.

[22] G. Acosta-Marum and M. A. Ingram, "Six time- and frequency-selective empirical channel models for vehicular wireless LANs," *IEEE Veh. Tech. Mag.*, vol. 2, no. 4, pp. 4–11, Dec. 2007.

[23] X. Cheng, C.-X. Wang, B. Ai, and H. Aggoune, "Envelope level crossing rate and average fade duration of non-isotropic vehicle-to-vehicle Ricean fading channels," *IEEE Trans. on Intell. Transp. Syst.*, vol. 15, no. 1, pp. 62-72, Feb. 2014.